Turbulent Heat Fluxes in Urban Areas: Observations and a Local-Scale Urban Meteorological Parameterization Scheme (LUMPS)

C. S. B. GRIMMOND

Atmospheric Science Program, Department of Geography, Indiana University, Bloomington, Indiana

T. R. OKE

Department of Geography, University of British Columbia, Vancouver, British Columbia, Canada

(Manuscript received 11 November 2001, in final form 2 February 2002)

ABSTRACT

A linked set of simple equations specifically designed to calculate heat fluxes for the urban environment is presented. This local-scale urban meteorological parameterization scheme (LUMPS), which has similarities to the hybrid plume dispersion model (HPDM) scheme, requires only standard meteorological observations and basic knowledge of surface cover. LUMPS is driven by net all-wave radiation. Heat storage by the urban fabric is parameterized from net all-wave radiation and surface cover information using the objective hysteresis model (OHM). The turbulent sensible and latent heat fluxes are calculated using the available energy and are partitioned using the approach of de Bruin and Holtslag, and Holtslag and van Ulden. A new scheme to define the Holtslag and van Ulden α and β parameters for urban environments is presented; α is empirically related to the plan fraction of the surface that is vegetated or irrigated, and a new urban value of β captures the observed delay in reversal of the sign of the sensible heat flux in the evening. LUMPS is evaluated using field observations collected in seven North American cities (Mexico City, Mexico; Miami, Florida; Tucson, Arizona; Los Angeles and Sacramento, California; Vancouver, British Columbia, Canada; and Chicago, Illinois). Performance is shown to be better than that for the standard HPDM preprocessor scheme. Most improvement derives from the inclusion of the OHM for the storage heat flux and the revised β coefficient. The scheme is expected to have broad utility in models used to calculate air pollution dispersion and the mixing depths of urban areas or to provide surface forcing for mesoscale models of urban regions.

1. Introduction

Knowledge of the surface sensible heat flux and atmospheric stability is a necessary prerequisite of models to calculate air pollution dispersion, urban mixing depth, and mesoscale airflow. On an operational basis, direct observation of these variables in cities is rare; therefore, it is necessary to parameterize the terms using more routinely measured data. Such parameterizations are included in meteorological preprocessors (e.g., Seibert et al. 2000; de Haan et al. 2001). Here we present a local-scale urban meteorological parameterization scheme (LUMPS), which consists of a series of linked equations that allow the storage (ΔQ_S), turbulent sensible (Q_H), and latent (Q_E) heat fluxes to be calculated (Fig. 1). The basic premise is that heat fluxes can be modeled using net all-wave radiation, simple information on surface cover (areas of vegetation, buildings, and impervious materials), morphometry (roughness element height and density), and standard weather observations (air temperature, humidity, wind speed, and pressure). The method has relatively limited data requirements yet is sophisticated enough to predict the spatial and temporal variability of heat fluxes known to occur within, and between, urban areas (Grimmond and Oke 2000).

In this paper, the nonradiative heat flux submodels of LUMPS are outlined and are evaluated using local-scale meteorological data collected in seven North American cities. These observations constitute a multicity urban hydrometeorological database (MUHD) (described in section 3), which has been generated to document the variability of local-scale surface heat fluxes in urban environments. The ''surface'' here is the top of a ''box,'' the height of which extends from a measurement level above the city down to a depth in the ground where the diurnal conductive heat flux ceases. By ''local scale'' we refer to horizontal areas of approximately 10^2–10^4 m on a side and to measurement heights in the inertial sublayer above the urban canopy and its roughness sublayer (Fig. 2). At this height and scale, we expect the microscale variability of atmospheric effects generated by individual houses and other surfaces to be integrated into a characteristic neighborhood response.

Corresponding author address: Sue Grimmond, Department of Geography, Student Building 104, 701 E. Kirkwood Ave., Indiana University, Bloomington, IN 47405-7100.
E-mail: grimmon@indiana.edu

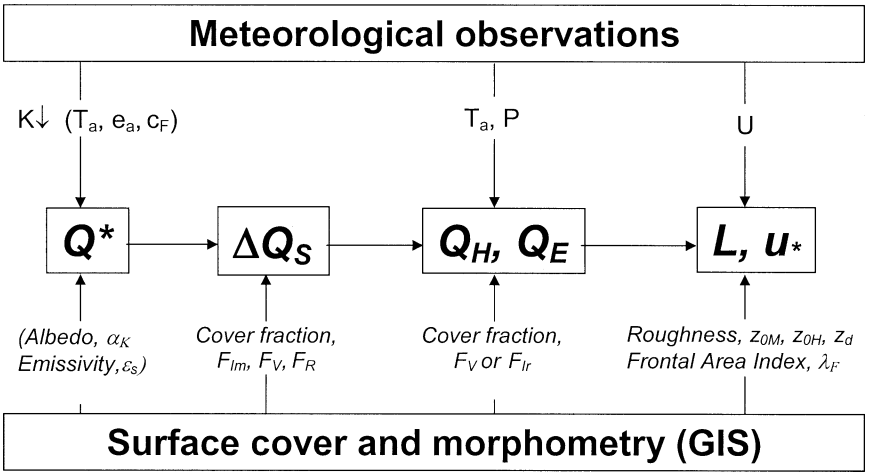

FIG. 1. Flow chart of the structure of LUMPS. Quantities in parentheses are needed only if net all-wave radiation Q^* or incoming shortwave radiation $K\downarrow$ are not measured: T_a is air temperature, e_a is actual vapor pressure, c_F is cloud fraction, P is pressure, U is wind speed, ΔQ_S is storage heat flux, Q_H is turbulent sensible heat flux density, Q_E is latent heat flux density, L is Obukhov length, and u^* is friction velocity.

The data in MUHD are used to derive parameters for LUMPS and to evaluate the fluxes the scheme predicts. We recognize that in so doing evaluation is not independent of model development. Further, the range of conditions for which LUMPS is applicable is limited to those in MUHD, particularly in terms of wind, surface moisture, and anthropogenic heat. Here, LUMPS is compared with relevant portions of the hybrid plume dispersion model (HPDM) urban preprocessor of Hanna and Chang (1992, 1993), which possesses several similarities.

2. The local-scale urban meteorological parameterization scheme

A flow chart of the structure of LUMPS (Fig. 1) shows that it is driven by relatively easily obtained meteorological and surface data. In this section, each submodel is described briefly. LUMPS is formulated in the framework of the surface energy balance (SEB),

$$Q^* = Q_H + Q_E + \Delta Q_S, \tag{1}$$

where Q^* is the net all-wave radiation. Here we are

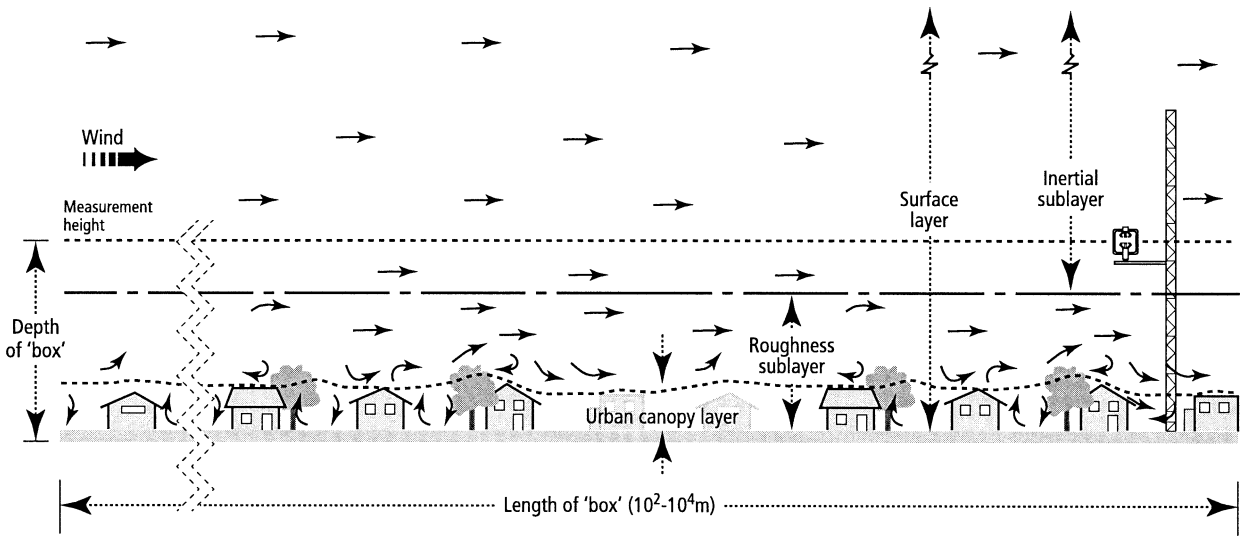

FIG. 2. Definition of layers involved in the study of urban climates at the local scale (modified after Oke 1997) relative to the box modeled by LUMPS. The lateral (or third) dimension of the box (not shown) is 10^2–10^4 m. Within the roughness sublayer (RSL) there is greater spatial variability of temporally averaged fluxes than within the inertial sublayer; i.e., these fluxes are chaotic in the urban canopy layer and RSL but become invariant in the inertial sublayer. The top of the box is within the inertial sublayer, and the bottom is at the depth at which there is no net heat exchange over the time period of interest.

TABLE 1 (a). Coefficients used to model storage heat flux [(2)]. Surface is divided into three surface types. The complete set of coefficients used for green space/open and paved/impervious surfaces is given in Table 4 of Grimmond and Oke (1999c). (b) Roof coefficients used with the OHM storage heat flux model from Meyn (2000).

Surface type	Sites where used	Basis for values	a_1	a_2 (h)	a_3 (W m^{-2})
(a) Coefficients used in current application					
Green space/open	All	Mean of all seven sources in Table 4 (Grimmond and Oke 1999c)	0.34	0.31	−31
Paved/impervious	All	Mean of all five sources in Table 4 (Grimmond and Oke 1999c)	0.70	0.33	−38
Rooftop	A93, A94 Sg94, S91u, Vs89, Vs92, T90	Mean of 9, 10, 11; see (b)	0.10	0.26	−4
	C95u	Mean of 9, 11; see (b)	0.11	0.30	−6
	Me93	Mean of 5, 8, 11, 12; see (b)	0.11	0.45	−8
	Mi95	Mean of 9, 10; see (b)	0.11	0.25	−4
	C92	Mean of 5, 8, 9, 11; see (b)	0.13	0.45	−9
	Vl92	Mean of 5, 8; see (b)	0.16	0.60	−12

(b) Roof type

	Code referred to in (a)	Source	a_1	a_2 (h)	a_3 (W m^{-2})
Vancouver (tar and gravel)	2	Yap (1973)	0.17	0.10	−17
Uppsala	3		Not recommended (Meyn 2000)		
Kyoto	4		Not recommended (Meyn 2000)		
Gravel, tar, concrete flat industrial (avg)	5	Meyn (2000)	0.25	0.92	−22
Gravel, tar, concrete flat industrial (dry)	6	Meyn (2000)	0.25	0.70	−22
Gravel, tar, concrete flat industrial (wet)	7	Meyn (2000)	0.25	0.70	−22
Bitumen spread over flat industrial membrane	8	Meyn (2000)	0.06	0.28	−3
Asphalt shingle–on-plywood residential roof	9	Meyn (2000)	0.14	0.33	−6
High-albedo asphalt shingle residential roof	10	Meyn (2000)	0.09	0.18	−1
Ceramic tile	11	Meyn (2000)	0.07	0.26	−6
Slate tile	12	Meyn (2000)	0.08	0.32	0

concerned primarily with the right-hand side of the SEB. Of interest are hourly fluxes, representative of the local scale (see section 1).

Net all-wave radiation sets the energetic bounds for the other fluxes in the surface energy balance. In the form of LUMPS presented and evaluated here, measured net allwave radiation is used to drive the scheme. In the absence of Q^* observations, this term can be obtained from parameterization using measured or modeled solar radiation $K\downarrow$ or a mixture of parameterization and modeling of the individual radiation fluxes (Newton 1999). If cloud is present, observation is greatly preferred.

In this paper, we restrict consideration to the energy balance fluxes in Fig. 1. Calculation of the friction velocity u^* and Obukhov stability length L will be addressed separately. Urban values of the roughness length for momentum and the zero-plane displacement have been addressed in Grimmond and Oke (1999a), and the roughness length for heat has been considered in Voogt and Grimmond (2000).

a. Storage heat flux

The storage heat flux in this urban SEB refers to the combined heat uptake and release from all substances (air, soil, biomass, and building materials) in the box, referred to as the equivalent surface flux through its top (Fig. 2). To capture the magnitude and diurnal hysteresis pattern of changes of the storage heat flux, the objective hysteresis model (OHM) of Grimmond et al. (1991) is used:

$$\Delta Q_S = \sum_{i=1}^{n} (f_i a_{1i}) Q^* + \sum_{i=1}^{n} (f_i a_{2i}) \left(\frac{\partial Q^*}{\partial t} \right) + \sum_{i=1}^{n} (f_i a_{3i}). \quad (2)$$

This requires knowledge of the local-scale net all-wave radiation, the fraction f of each of the n surface types within the area of interest, and the corresponding three coefficients (a_1–a_3; Table 1; see also Table 4 in Grimmond and Oke 1999c). The fraction of the surface occupied by each surface type can be calculated for a 2D (plan) or 3D (complete) area. Grimmond and Oke (1999c) conclude that incorporating 3D effects does not result in a significant improvement in the performance of OHM. Therefore for LUMPS at this stage, we recommend using the simplest surface description—that is, only the plan area of the impervious surfaces and rooftops—and combining the remaining green space and bare-ground areas into one category [thus, $n = 3$ in (2)]. Meyn (2000) provides new data for a_1–a_3 coefficients for roofs (Table 1b). These are incorporated into the version of OHM presented here.

TABLE 2. Previously quoted values of the α and β parameters: (a) range listed by Hanna and Chang (1992) based on information in Beljaars and Holtslag (1989, 1991) and (b) values for urban terrain used by Hanna and Chang (1992).

	α	β (W m^{-2})
(a) Range of values for all surface types		
Dry desert with no rain for months	0.0–0.2	20
Arid rural area	0.2–0.4	20
Crops and field, midsummer during periods when rain has not fallen for several days	0.4–0.6	20
Urban environment, some parks	0.5–1.0	20
Crops, fields or forests with sufficient soil moisture	0.8–1.2	20
Large lake or ocean with land more than 10 km distant	1.2–1.4	20
(b) Values selected for specific urban sites		
St. Louis (site-105 urban commercial, including warehousing and light industrial uses; plan area 25% buildings, 59% paved, 15% grass, 1% trees)	0.5	20
Industrial (''urban-tower'' site, grassy field adjacent to densely built-up area)	0.5	20

b. Sensible and latent heat flux

In formulating their HPDM, Hanna and Chang (1992, 1993) use the parameterizations of the turbulent sensible and latent heat fluxes (Q_H and Q_E, respectively) proposed by de Bruin and Holtslag (1982). When written in a form appropriate for an urban environment, these are

$$Q_H = \frac{(1 - \alpha) + (\gamma/s)}{1 + (\gamma/s)}(Q^* - \Delta Q_S) - \beta \quad \text{and} \quad (3)$$

$$Q_E = \frac{\alpha}{1 + (\gamma/s)}(Q^* - \Delta Q_S) + \beta, \quad (4)$$

where s is the slope of the saturation vapor pressure–versus-temperature curve, γ is the psychrometric ''constant,'' and α and β are empirical parameters. These parameters are based on a simplification of the Penman–Monteith approach, which takes into account the Priestley–Taylor coefficient α_{PT} for extensive wet surfaces but extends it to include nonsaturated areas. To evaluate (3) and (4), the two parameters α and β must be specified. The α parameter accounts for the strong correlation of Q_H and Q_E with $Q^* - \Delta Q_S$, whereas β accounts for the uncorrelated portion (Holtslag and van Ulden 1983). As noted, α depends on the surface moisture status, and in the original scheme β was an empirical constant. Table 2, taken from Hanna and Chang (1992), summarizes their default guidance values for these parameters for a range of land cover conditions.

Holtslag and van Ulden (1983) outline a method to determine the α and β parameters that involves rewriting (4) as

$$Q_E = \alpha\left[\frac{1}{1 + (\gamma/s)}(Q^* - \Delta Q_S) + \beta'\right], \quad (5)$$

where β' is the value for which $\alpha = 1$, given that $\beta = \alpha = 0$ when $Q_E = 0$ W m^{-2}, and $\beta = \beta'\alpha$. Using (5) and measurements of Q_E (with Q^*, ΔQ_S, and temperature to determine s and γ), the parameters can be derived from regression analysis; α then can be related to the moisture status of the surface (Holtslag and van Ulden 1983), and predictive relations can be developed. Holtslag and van Ulden (1983) indicate that a value of $\beta = 20$ W m^{-2} is reasonable, and this value has been used subsequently by others (Table 2). Hanna and Chang (1992) note that the use of a constant β accounts for the observation that Q_H turns negative before sunset. However, they do not back-calculate values for either of the parameters from their urban data for use in HPDM. Here we investigate both parameters based on our emerging understanding of flux partitioning in urban environments (see section 3c).

c. Anthropogenic heat

Similar to the energy balance formulation of HPDM, we do not include an anthropogenic heat flux Q_F. For the range of conditions we consider (see further descriptions below) and the approach we adopt, we do not think it is necessary. This is a saving in input requirements and uncertainty. LUMPS is based on a *measured*, not a theoretical or modeled, surface energy balance. The instruments used to measure Q^*, Q_H, and Q_E are likely to sense most of the anthropogenic contributions to the radiative, convective, and conductive fluxes. Parameterized terms based on these *measured* quantities thus already include the effects of Q_F. Adding an independent anthropogenic heat term would be ''double counting'' this heat source. We stress, however, that this approach is only valid for the range of conditions so far encountered in MUHD, the observational base of the parameterization. MUHD is biased toward low-density residential areas in summer. It will be necessary to extend MUHD to include observations from sites at which Q_F is large or to devise other modifications to the LUMPS relations if it is to be applied at sites at which combustion release is very large (e.g., manufacturing

areas or high-rise residential or commercial complexes), especially if they are cities located in extremely hot or cold climates with significant space cooling or heating.

3. The multicity urban hydrometeorological database

a. The sites

This section outlines the methods and results of work we have conducted over the last decade to compile a multicity urban hydrometeorological database. To date we have observed fluxes and climate data at 10 sites in seven North American cities, and at 2 of the sites we have data for two different periods (see Table 3). These data have informed our understanding of flux partitioning in urban environments and are used here to evaluate parameterizations of the turbulent sensible and latent heat fluxes. The construction of this database is ongoing, and field campaigns are under way and planned at additional sites to enhance the range of surface and atmospheric conditions sampled and also to provide independent test sets.

Each set of observations in MUHD is identified by its geographic location (one- or two-letter code) and the year in which it was conducted (last two digits). The sites, selected to represent different building styles and climates, range from Vancouver, British Columbia, Canada, (Vl92, Vs92) in the northwest of North America to Mexico City, Mexico, (Me93) in the south. There are observations from the dry southwestern region of the United States (Tucson, Arizona, T90; Los Angeles, California, A93, A94, Sg94; Sacramento, California, S91) and from the more humid Great Lakes (Chicago, Illinois, C95) and subtropical southeastern region (Miami, Florida, Mi95). The data were collected in the summertime, with the exception of Mexico City, for which observations were conducted during the dry season (December of 1993).

Most of the data were collected in short-campaign (1–8 weeks) field programs. Simultaneous observations were made at two different locations within both Los Angeles (A94 and Sg94) and Vancouver (Vs92 and Vl92). In addition, data were collected at the same site in Los Angeles in two consecutive summers (A93 and A94) and in Vancouver (site Vs) in 1989 and 1992. In Chicago, measurements were made in two closely proximate neighborhoods in 1992 and 1995 (C92 and C95). In general, Chicago was windy and moist, Tucson was hot and dry with strong daily wind variations, and Sacramento and Los Angeles were dry with a weak wind in the afternoon. Except for Chicago and Miami, the measurement periods were predominantly rain free.

For each of the sites, geographic information systems (GIS), spatially georeferenced databases, have been created to archive data about the surface cover and building/vegetation morphometry surrounding the measurement site (Grimmond and Souch 1994). These data pro-

TABLE 3. Study sites ordered by decreasing fraction of the surface built (combined area of roofs and impervious surfaces, or conversely, increasing fraction green space). Code refers to the location and year of observation, e.g., Me93 refers to Mexico City in 1993. Land use: suburban (Sub), light industrial (LI), downtown/central (D). Urban terrain zones (UTZ) according to Ellefsen (1990–91). Fraction plan area: buildings (Bld), impervious (Imp), unmanaged or vacant (UM), trees (TR), grass (GR), or water (WT) (after Grimmond and Oke 1999b).

Site	Code	Obs period	Original reference with full details	Height of buildings: mean and std dev	Land/Use and UTZ	Land cover (plan-area fraction)					
						Bld	Imp	UM	TR	GR	WT
Mexico City	Me93	Dec 1993	Oke et al. (1999)	18.4 ± 6.6	D/A2	54	44	2	1	0	0
Vancouver, BC	Vl92	Aug 1992	Grimmond and Oke (1999c)	5.8 ± 0.1	LI/Do4	51	44	0	3	2	0
Tucson, AZ	T90u	Jun 1990	Grimmond and Oke (1995)	5.2 ± 0.8	Sub/Do3	23	42	17	11	7	0
Miami, FL	Mi95	May/Jun 1995	Newton (1999)	8.0 ± 2.1	Sub/Do3	35	29	0	7	27	2
Chicago, IL	C95	Jun/Aug 1995	King and Grimmond (1997)	5.9 ± 1.3	Sub/Dc3	36	25	0	7	32	0
San Gabriel, Los Angeles, CA	Sg94	Jul 1994	Grimmond et al. (1996)	4.7 ± 0.2	Sub/Do3	29	31	0	12	25	4
Chicago, IL	C92	Jul 1992	Grimmond et al. (1994)	6.7 ± 0.5	Sub/Do3	33	22	1	10	34	0
Vancouver, BC	Vs92	Jul/Sep 1992	Grimmond and Oke (1999c)	4.7 ± 0.2	Sub/Do3	31	23	2	9	35	0
Vancouver, BC	Vs89	Jul 1989	Roth and Oke (1993)	4.7 ± 0.2	Sub/Do3	31	23	2	9	35	0
Sacramento, CA	S91u	Aug 1991	Grimmond et al. (1993)	4.8 ± 0.2	Sub/Do3	36	12	1	13	34	5
Arcadia, Los Angeles, CA	A94	Jul 1994	Grimmond et al. (1996)	5.2 ± 0.2	Sub/Do3	24	19	2	30	23	2
Arcadia, Los Angeles, CA	A93	Jul/Aug 1993	Grimmond and Oke (1995)	5.2 ± 0.2	Sub/Do3	22	18	2	32	24	2

vide information on the average height of the roughness elements (buildings and trees), their horizontal dimensions, their spacing, and the fraction of the area they cover. The urban land uses represented include central city (old colonial core of Mexico City, Me93), light industrial (one- and two-story warehouses in Vancouver, Vl92), and low- or medium-density residential housing (the remainder of the sites). The land cover varies from less than 5% vegetated (Me93, Vl92) to a residential area with almost 60% vegetation cover (Los Angeles, A93, A94; Table 3). Across all sites, the buildings vary in height from 5 to 19 m (Table 3). At many of the residential sites, the trees are as tall or taller than the houses.

The surface moisture availability at the MUHD sites varied greatly, and this is critical to their characteristic energy partitioning. Given the infrequent rainfall in Tucson, Sacramento, and Los Angeles, the vegetation in the neighborhoods surrounding the measurement sites can only be maintained by irrigation. In Los Angeles and Sacramento, plentiful irrigation sustains lush green landscapes. In Sacramento during the observation period, people living in the vicinity of the site were permitted to irrigate on alternate days of the week depending on their street address (i.e., alternation of odd- and even-numbered houses). Watering was not permitted on Sundays. In Los Angeles, no regulations were imposed on irrigation, and frequent watering occurred in the early morning and late afternoon (Grimmond et al. 1996). In Tucson, on the other hand, where water conservation is encouraged, the vegetation is xeric. A reasonable amount of biomass is present, but it is adapted to an environment in which water is a limiting factor. Much of the irrigation occurs at night as drip or subsurface irrigation for short periods and in a much more targeted manner than in the other cities. In Vancouver, which experiences mild summer drought, there is normally (e.g., Vs89) considerable sprinkler-type irrigation of gardens and parks. In 1992, however, lack of precipitation led to a ban on external irrigation, so the residential area (Vs92) was much drier than normal.

b. Atmospheric observations

The surface energy balance data contained within MUHD are observations made using instruments mounted on tall towers (18–45+ m), usually at heights of at least 2 times the mean height of the roughness elements. This measurement height ensures that the instruments are above the influence of individual roughness elements and that the fluxes observed represent an integrated response at the local scale (Grimmond and Oke 1999a,c; Rotach 2000). At the instrument heights used, the source areas for the radiation measurements are approximately 5–12 $\times$ 10^4 m^2 (i.e., circles of radius 125–195 m centered on the tower). The elliptically shaped source areas for the turbulent fluxes, which lie upwind of the tower sites, range from approximately 1.5 $\times$ 10^5 to 5 $\times$ 10^6 m^2 depending on stability, roughness, and wind speed [for typical shapes, see Schmid (1994)].

At each site, a net radiometer has been used to measure net allwave radiation flux density, a sonic anemometer–thermometer system has been used to measure the turbulent sensible heat flux density, and a krypton hygrometer (with the sonic anemometer) has been used to measure the latent heat flux density. Hence, the turbulent heat fluxes are directly measured by eddy covariance, and heat storage change in the urban fabric, expressed as a heat flux density through a horizontal plane (Fig. 2), is found as the residual in the surface energy balance (which therefore accumulates all measurement errors and neglected terms). Grimmond and Oke (1999b,c) provide fuller details about the instrumentation, its exposure, and the postprocessing of data. Results are hourly averages corrected to local apparent time (LAT) to ensure consistency of solar noon. Daytime and nighttime are defined herein as the times during which Q^* is positive or negative, respectively, and ''daily'' means the 24-h period.

c. Summary of known flux partitioning in urban environments

Detailed descriptions of the fluxes and flux partitioning measured as part of MUHD are presented elsewhere (see references in Table 3). The turbulent and storage heat fluxes all represent important terms in the surface energy balance of urban environments. Here we summarize the most important characteristics of these fluxes, focusing on their magnitude, variability, and diurnal course, and the implications for the parameterizations used in LUMPS.

1) STORAGE HEAT FLUX

For the sites and conditions considered in MUHD, the heat added to or removed from the fabric of the buildings, roads, trees, ground, and the air in the layer beneath measurement level is most important at the downtown and light-industrial sites. At such dry and built-over sites, heat storage changes sequester at least 50% of daytime Q^*. Here ΔQ_S is typically 20%–30% of daytime Q^* at residential sites (Grimmond and Oke 1999c). Average peak daily values range from approximately 150 to 280 W m^{-2} (Fig. 3), considerably larger than for most natural systems, except water. At night the release of the daytime heat reservoir produces an upward-directed flux that is initially larger than the net radiation. Then, after one or two hours it settles into a remarkably simple pattern in which it is within $\pm$5% of the net radiation loss.

At the hourly timescale and from day to day, ΔQ_S is variable [see examples presented in Grimmond and Oke (1999c)]. Some of this variability can be attributed to differences in radiant loading; however, even on cloud-

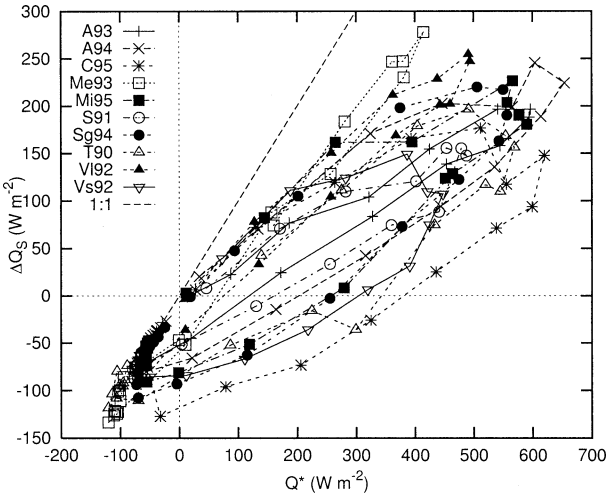

FIG. 3. Mean diurnal hysteresis pattern between observed urban heat storage change (ΔQ_S) and net all-wave radiation (Q^*). Individual hysteresis patterns are shown in Grimmond and Oke (1999c). (Note that Figs. 3–8 contain no Vs89 results because of insufficient data to calculate ensemble means.)

free days, when the diurnal pattern of Q^* is smooth, hourly variability results from variations in the convective fluxes (see further discussion below).

Storage heat flux uptake in urban areas is not symmetrical around solar noon; rather, there is a distinct tendency for more energy to enter the urban fabric in the morning (Fig. 3). This hysteresis pattern suggests that parameterizing ΔQ_S as a fixed fraction of Q^* (e.g., as in HPDM) is less appropriate than a scheme that takes this diurnal hysteresis pattern into account (see section 2a). For most of the night, however, it is acceptable to equate ΔQ_S approximately to Q^*.

2) LATENT HEAT FLUX

Figure 4 summarizes the latent heat fluxes for each of the datasets. The average daily maximum latent heat flux in summertime varies between 10 and 235 W m^{-2} (Fig. 4a). It is not a surprise that those areas with little vegetation (downtown Me93 and industrial Vl92) have extremely small latent heat flux values (Grimmond and Oke 1999b). The very low value ($\sim$10 W m^{-2}) at Me93 is partly due to the low radiation input in winter but is unlikely to be much greater in summer unless the surface is wetted by rain. Of the residential sites, Vancouver (Vs92) has the lowest rates. As mentioned, the 1992 observations for Vancouver are atypical, based on comparisons with previous work (Cleugh and Oke 1986; Grimmond 1992), because of abnormally dry conditions that summer and a very effective ban on garden irrigation (Smith 1994). Vegetation that normally receives large amounts of external irrigation supplemented by occasional rainfall (Grimmond and Oke 1986) was water stressed and had little evaporation.

The other residential areas have daytime peaks in evapotranspiration that range from 125 to 235 W m^{-2}. On average at the residential sites, Q_E constitutes an energy sink of 22%–37% of daytime and 28%–46% of daily net all-wave radiation. Those areas receiving greater irrigation or precipitation have greater rates of evapotranspiration on average (Grimmond and Oke 1999b).

Figure 4b gives a sense of the hour-to-hour and day-to-day variability of Q_E at two of the sites, Chicago (C95) and Los Angeles (A94), both of which have higher-than-average evapotranspiration rates. C95, where water is supplied by frequent rain events and irrigation, has greater variability. At A94, the data are more consistent from day to day because of automated irrigation systems, which give a fairly constant supply of water, and the relatively constant synoptic conditions. This consistency also is evident at the site between years (see A93, A94).

Despite the surface and soil moisture supplied by garden irrigation that helps to maintain these evaporation rates, all of the urban evapotranspiration fluxes fall below equilibrium rates $\{Q_{E\mathrm{eq}} = (Q^* - \Delta Q_S)[s/(s + \gamma)]\}$ during the daytime (Fig. 4c). This fact is presumably due to the presence of dry surfaces, especially built surfaces, within the flux source areas. Variability is evident between sites in the early morning. This is attributable to differences in the occurrence or abundance of dewfall and nocturnal irrigation. By late afternoon, Q_E is more similar between the sites [for further discussion, see Grimmond and Oke (1999b)].

As may be anticipated, there are overall relations between measures of surface cover, such as the fraction of green space or area irrigated at each site, and the Q_E fluxes (when normalized by Q^*, or represented as a fraction of the total turbulent transport, the Bowen ratio Q_H/Q_E; Fig. 5).

3) SENSIBLE HEAT FLUX

The average daily maximum sensible heat flux in the MUHD summertime sets (i.e., excluding Me93) varies between 200 and 300 W m^{-2} (Fig. 6a). Unlike the case of Q_E, there are no cities with extremely small Q_H, because heat, unlike water, is available everywhere at the surface. At all the residential sites, the sensible heat flux is numerically the most important heat sink in the surface energy balance, ranging from $\sim$40% to 60% of daytime Q^*. At the light-industrial site (Vl92), Q_H represents approximately 40% of Q^*, but at this dry (low Q_E) site, ΔQ_S is a greater heat sink than Q_H by day. The smallest daytime maximum Q_H occurs in the driest of all the sites, Mexico City. However, this low convective flux is partly explained by the fact these are winter data. It is also consistent to note the significance of the large heat storage by the massive old colonial buildings (Oke et al. 1999). Notice that, when normalized by Q^*, the role of Q_H in Me93 is the lowest of all cities (Fig. 6b).

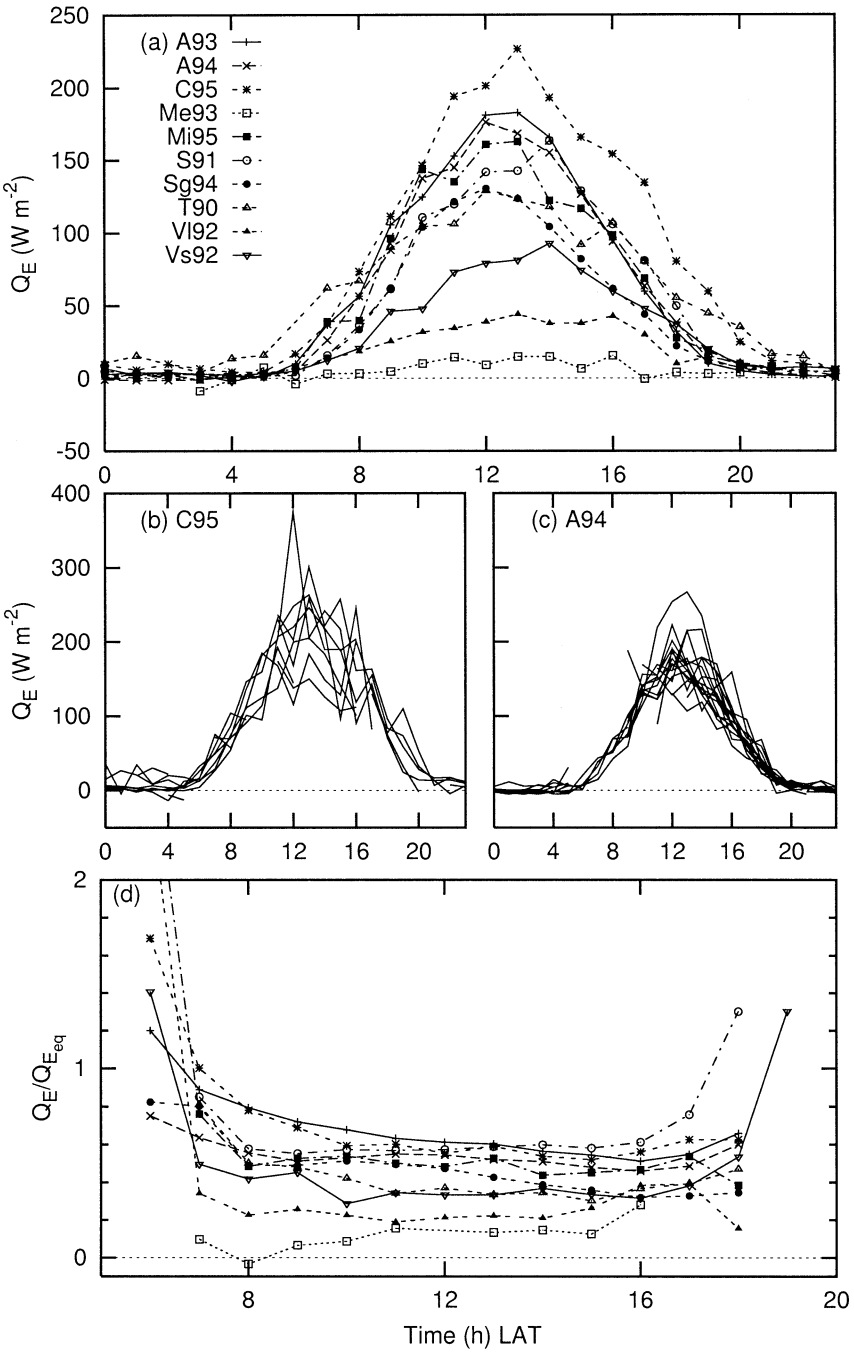

FIG. 4. Diurnal patterns of latent heat flux: (a) ensemble mean patterns in MUHD cities, individual daily data for (b) Chicago (C95) and (c) Arcadia, California, (A94) to illustrate variability from day to day, and (d) average measured Q_E as a fraction of equilibrium Q_{Eeq} (modified from Grimmond and Oke 1999b). See Table 3 for time period of observations and surface characteristics of sites.

All sites shed more energy as sensible heat than as latent heat, that is, Bowen ratios are greater than 1 (Fig. 5c). Daytime Bowen-ratio values for the residential sites range from approximately 1.2 to 2, except for Vs92 ratios, which climb to ~2.8 during the irrigation ban. The average daytime Bowen ratio at the sparsely vegetated light-industrial site (Vl92) is ~4.4, and in central Mexico City it reaches ~9.8.

In an absolute sense there is not much variability in Q_H at night anywhere, although the sign of the flux does vary between sites (Fig. 6a). When normalized by Q^*, the variability appears greater (Fig. 6b), but this is in part due to creating a ratio from small numbers. Of particular interest, however, is the time in the evening when Q_H turns negative. At rural sites, this regularly happens before sunset as the radiative inversion be-

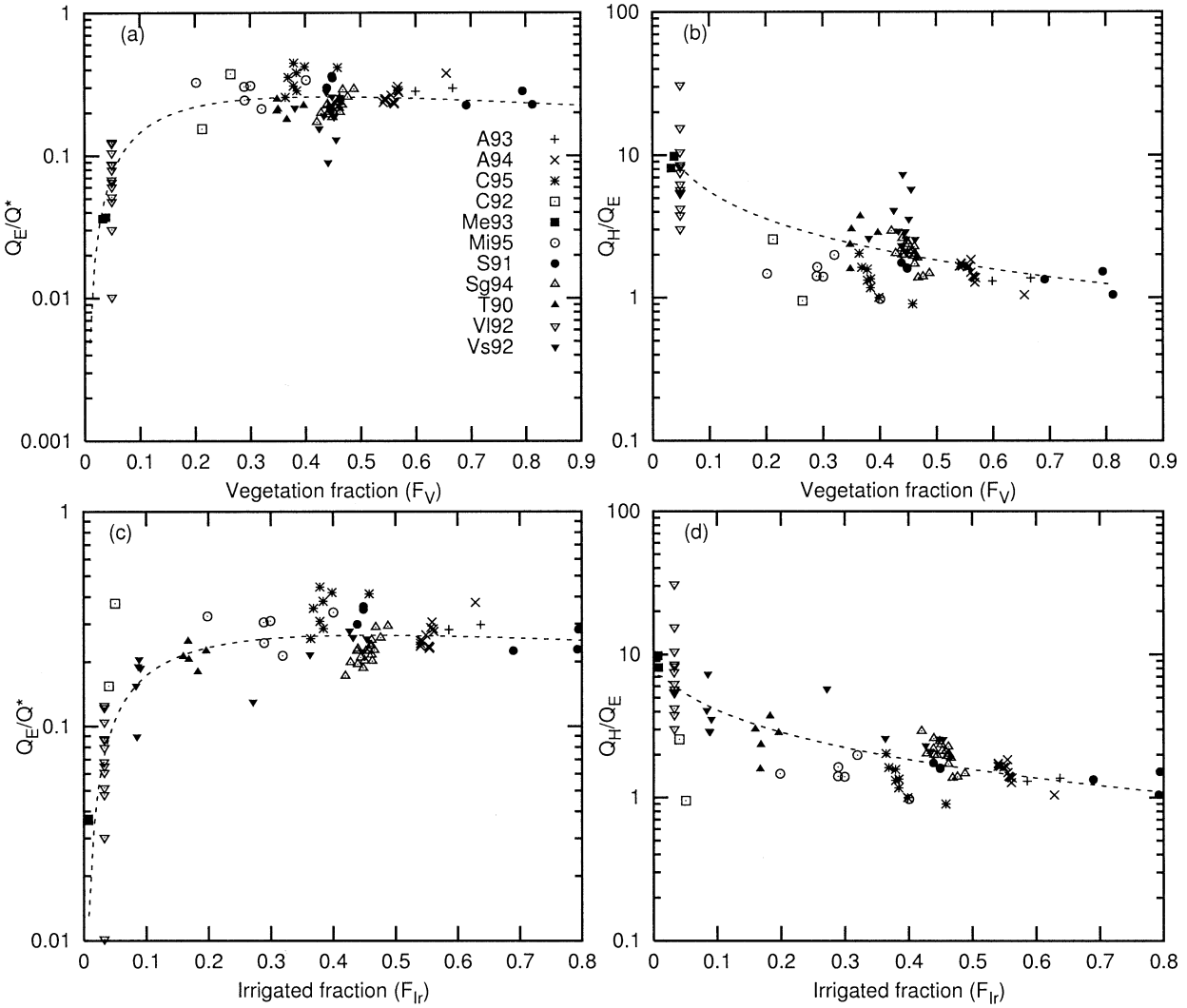

FIG. 5. Relations between (a) Q_E/Q^* and fraction of plan area that is vegetated (F_V), (b) Bowen ratio (Q_H/Q_E) and F_V, (c) Q_E/Q^* and fraction of plan area that is irrigated (F_{Ir}), and (d) Q_H/Q_E and F_{Ir} for all MUHD cities. Data plotted are for individual 4-h periods between 1000 and 1400 LAT when there was consistent fetch.

comes established. On this basis, Holtslag and van Ulden, and others since (section 2c), propose the use of a constant β parameter (typically set to 20 W m^{-2}; Table 2) in (3) and (4). On the other hand, our data, and that of others from fully urbanized sites (Oke 1988), show a different pattern wherein Q_H tends to remain positive after sunset, sometimes for several hours, even throughout the night. This behavior suggests that β values for cities may be different from those of rural sites. Figure 7 shows the ensemble mean ratio Q_H/Q^* for each site for the period when Q^* is negative (starting at 1 on the time axis until the time when it turns positive the next day, 2 on the x axis). The time axis is normalized so that the effect of different night lengths is removed. At all sites, Q_H turns negative well after Q^*, if at all. This result is thought to be due to the large release of heat storage, the radiative screening and shelter effects of canyon geometry, and the release of Q_F from traffic and buildings.

4. Parameters for LUMPS based on MUHD

As noted, the turbulent sensible and latent heat fluxes can be modeled using the simple approach of de Bruin and Holtslag (1982). Here we back-calculate the α and β coefficients for each of our sites using our measured latent heat fluxes and the other measured data necessary to solve (5). Calculations are conducted on an hourly basis and are restricted to any hour during a day during which the fetch direction and therefore the turbulent source area were steady for the complete hour. Surface cover, notably the plan area (fraction) covered by vegetation F_V and the area irrigated F_{Ir} in the source area, is calculated following the procedure outlined in Grim-

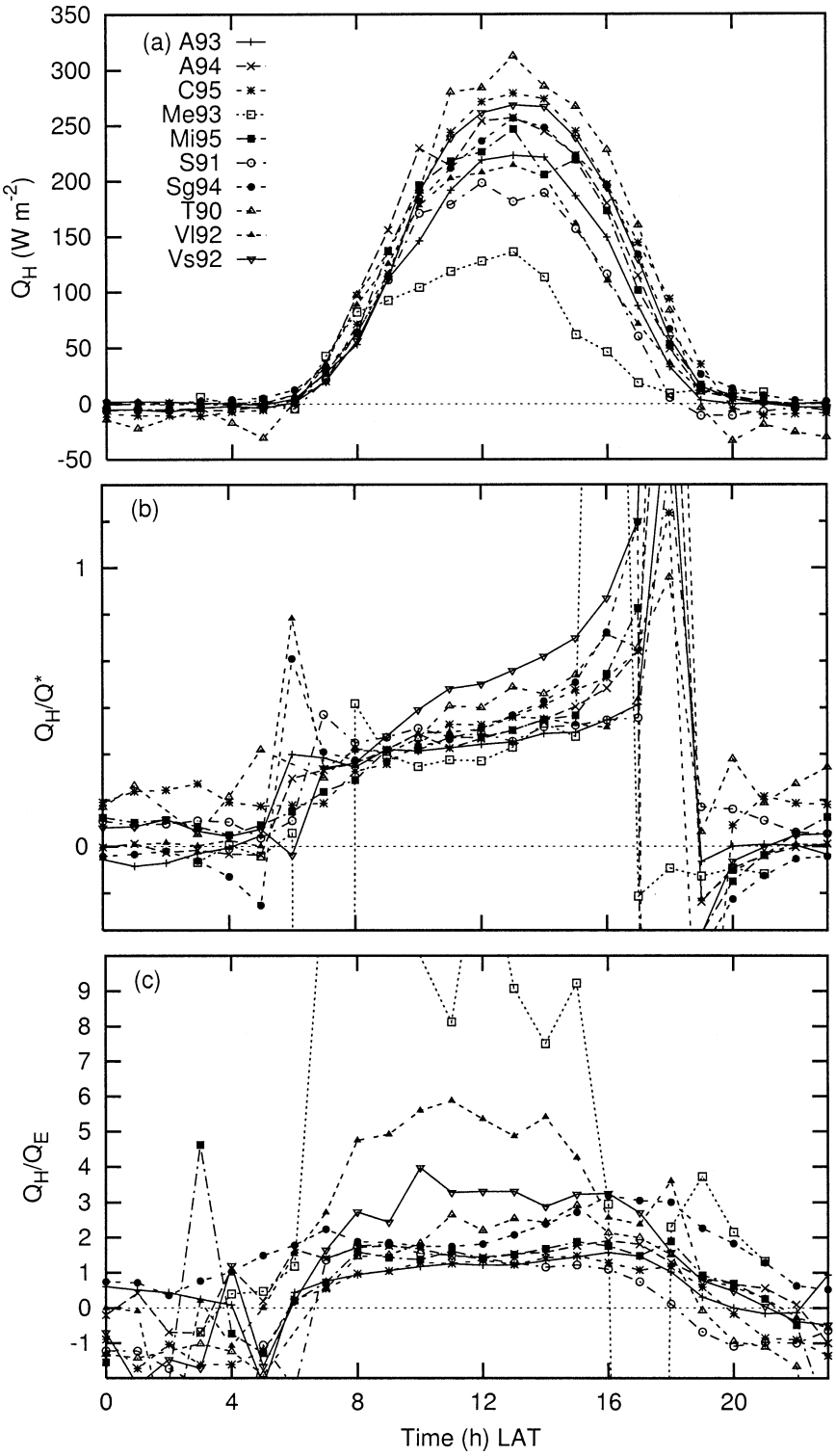

FIG. 6. Diurnal patterns of (a) ensemble mean turbulent sensible heat flux density (W m^{-2}), (b) ensemble mean Q_H/Q^*, and (c) ensemble mean Bowen ratio (Q_H/Q_E) for MUHD cities.

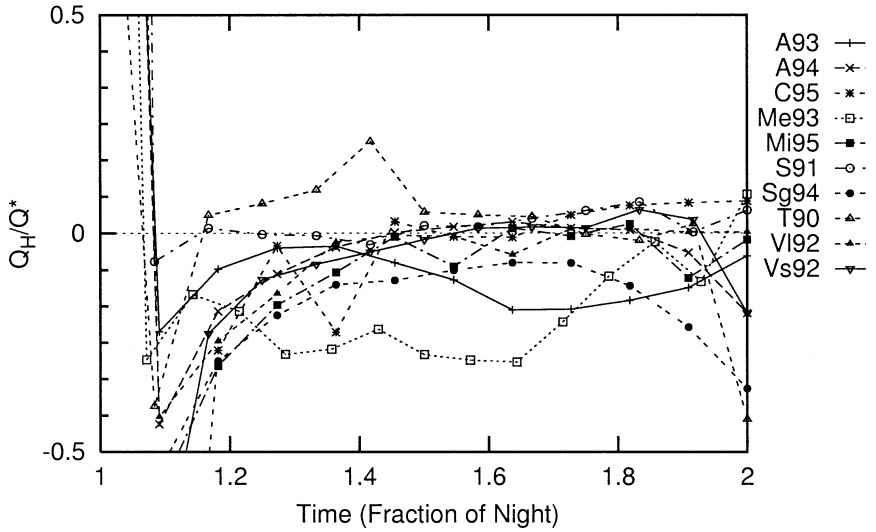

FIG. 7. Variation of nocturnal turbulent sensible heat flux normalized by net all-wave radiation (Q_H/Q^*). Time on the horizontal axis is standardized for all sites so that the time when Q^* becomes negative is 1 and it becomes 2 when it turns positive again.

mond and Souch (1994). These cover fractions are then correlated with the corresponding α and β coefficients to identify any statistically meaningful relations (Holtslag and van Ulden 1983).

The back-calculated α values range from less than 0.2 to greater than 0.7 for the sites considered here (Table 4). One-half of the α values are lower than those previously suggested as appropriate for urban areas (Table 2). All of the poorly vegetated sites or those experiencing some form of drought have particularly low values. This fact becomes clear when the α values are plotted against the average area of vegetated surfaces in the source area (footprint) of the turbulent heat flux measurements (Fig. 8a). The vegetated fraction (F_V, the plan area covered by grass, trees, shrubs, and open water) is used as a descriptor to be consistent with the objective of keeping model inputs as simple as possible (such data can be generated easily from analysis of aerial photographs). Those sites that lie above the general trend line (Chicago and Miami) are locations with above-average surface water availability, because of frequent rainfall and/or extensive irrigation (Grimmond and Oke 1999b) or because of canals (Newton 1999). Those sites that plot below the line tend to be areas in which irrigation is restricted, notably the residential area in Vancouver (Vs92), which was under an irrigation ban. When the plan-area fraction of irrigated cover is used, which is a more direct measure of surface moisture status, the scatter in the relation is reduced (Fig. 8b and Table 5). In this study, values of F_{Ir} were assessed from aerial photographs and field surveys. If infrared surveys or other appropriate remotely sensed data were available, they would help to refine such estimates. For periods of rainfall (not considered here) when the surface is wet, F_{Ir} should be set to 1.0.

TABLE 4. Average β (W m^{-2}) and α values for each site ordered by decreasing size of β.

Site	City	β (W m^{-2})	α
T90	Tucson	8.4	0.28
C95	Chicago	6.6	0.58
C92	Chicago	5.6	0.71
S91	Sacramento	2.9	0.56
Vs89	Vancouver	2.3	0.43
Mi95	Miami	2.3	0.51
A93	Arcadia, Los Angeles	2.2	0.57
Vs92	Vancouver	1.5	0.35
A94	Arcadia, Los Angeles	1.2	0.51
Vl92	Vancouver	0.6	0.22
Sg94	San Gabriel, Los Angeles	0.3	0.43
Me93	Mexico City	−0.3	0.19
Mean		2.8	0.45

The influence of surface cover on the α parameter can be considered in more detail by extending the analysis to incorporate the complete range of surface cover information contained in the measurements for each site. Variations in surface cover around each site and changes in wind direction, wind speed, and atmospheric stability combine to create a spectrum of different turbulent source areas for the same site. Utilizing these multiple samples increases the range of conditions over which relations between α and F_V and F_{Ir} can be established and thereby allows us to consider how such relations hold up both *within*, as well as *between*, urban areas.

Data for each hour for each site were stratified into classes based on the land cover of the sampled turbulent flux source area. In the example reported here, land cover classes of 5% (i.e., 0%–5%, 5%–10%, and 10%–15% of plan area vegetated or irrigated) were used. For those land cover classes with at least 25 observations, the measured latent heat fluxes were used to back-calculate α and β coefficients. These values, in turn, were plotted against the average surface cover (Figs. 8c,d).

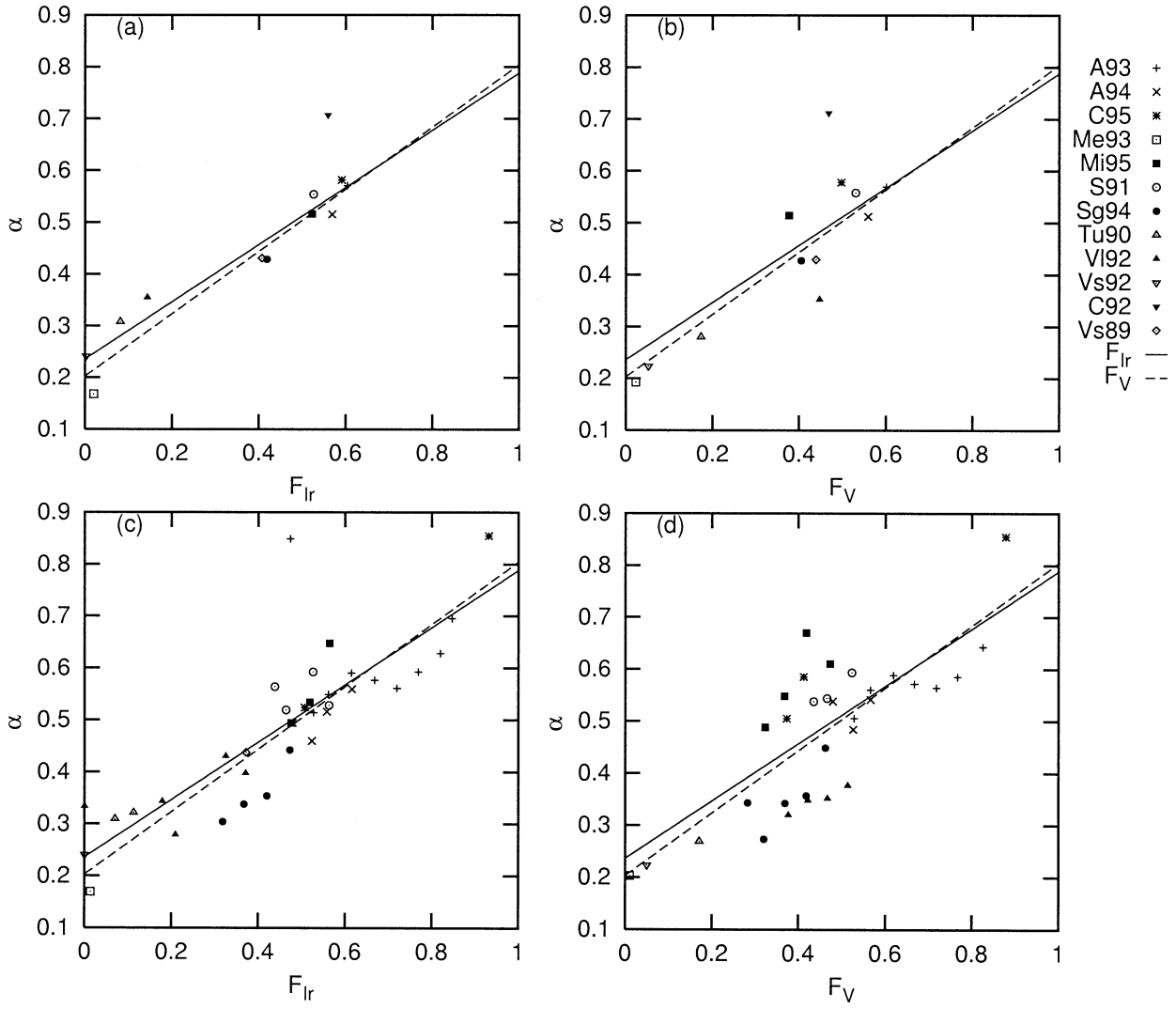

FIG. 8. Relation between surface characteristics (F_{Ir} and F_V) and α coefficients (a), (b) determined as averages for each site and (c), (d) for multiple land cover categories for each site.

The relations between α and both measures of surface cover (F_V and F_{Ir}) are good, but again correlations are much stronger with F_{Ir} (Table 5). Urban areas with similar plan-area vegetated cover are not identical, because they encompass a range of surface moisture conditions. It is interesting to note on Figs. 8c,d that, for all cities, as the fraction vegetated or irrigated in the turbulent source area increases, so too does the α parameter. This result suggests that this is an appropriate approach for assigning variations in the α parameter to simulate spatial variability in turbulent heat fluxes *across* a city as well as *between* cities.

TABLE 5. Relation between α coefficient and land cover (LC) characteristics: n is the number of points available for developing the relation, rmse (W m^{-2}), rmse$_{sy}$ (systematic) and rmse$_{usy}$ (unsystematic), r^2 is coefficient of determination, F_{Ir} is the fraction of the plan area irrigated, and F_V is the fraction of the plan area vegetated. See text for further details.

	n	Slope	Intercept	r^2	Rmse	Rmse$_{sy}$	Rmse$_{usy}$
Avg for each site							
F_V	12	0.686	0.189	0.699	0.123	0.091	0.082
F_{Ir}	12	0.610	0.222	0.863	0.130	0.118	0.056
5% LC class							
F_V	37	0.596	0.220	0.500	0.143	0.087	0.114
F_{Ir}	37	0.547	0.239	0.715	0.138	0.112	0.081

TABLE 6. Conditions used in runs of LUMPS to evaluate effects of changing α, β, and ΔQs independently. The rmse (W m^{-2}) is presented as a summary of the results. Fuller details of model performance by city for select runs are presented in Figs. 9 (run 7), 10 (run 5), and 11 (run 11). Run 13 represents average conditions for site used in calculation for all hours. The n for each site is given in Fig. 9a.

	Runs												
Options	1	2	3	4	5	6	7	8	9	10	11	12	13
Model							HPDM	HPDM			LUMPS	LUMPS	LUMPS
Q^*	← Measured →						← 0.3Q^* →				← Eq. (2) →		
ΔQs													
α	0.5	1.0	$f(F_v)$	$f(F_{lr})$	$f(F_V)$	$f(F_{lr})$	0.5	1.0	$f(F_V)$	$f(F_{lr})$	$f(F_V)$	$f(F_{lr})$	$f(F_V)$
β (W m^{-2}	20	20	20	20	3	3	20	20	3	3	3	3	3
Summary results (for 12 sites), observed mean (W m^{-2}) Q_H = 79, Q_E = 51, ΔQ_s = 20													
$\overline{\text{Rmse}}$ (W m^{-2})													
Q_H	30	88	26	24	20	19	57	94	51	49	41	39	42
Q_E	30	88	26	24	20	19	36	93	30	30	27	27	27
ΔQs	—	—	—	—	—	—	68	68	68	68	53	53	53
$\overline{\text{Rmse}}_{sy}$ (W m^{-2})													
Q_H	23	88	18	17	12	9	37	92	25	23	23	21	22
Q_E	24	80	19	18	12	10	19	69	16	15	16	15	16
ΔQs	—	—	—	—	—	—	59	59	59	59	28	28	28
$\overline{\text{Rmse}}_{usy}$ (W m^{-2})													
Q_H	16	8	16	15	16	15	41	18	42	42	32	32	34
Q_E	18	36	16	15	15	15	29	58	25	25	21	20	20
ΔQs	—	—	—	—	—	—	32	32	32	32	43	43	43

The back-calculated β values from the analysis of all sites are given in Table 4. The values are significantly smaller than the 20 W m^{-2} figure suggested for rural sites. This is as expected given the diurnal course of Q_H that includes a delay, or complete failure, to turn negative at night (Fig. 7). Unlike the α coefficients, however, there is no obvious relation between β and measures of surface cover. Tucson and Chicago have the largest β values, but there is little to suggest why they should be similar, nor why downtown Mexico City and residential San Gabriel, California, should share some different ability with respect to the nocturnal transition period. However, it is important to stress that the overall range is small (0–9 W m^{-2}). At this stage, in the absence of an objective method to assign β values to different sites, we recommend a constant value of ~3 W m^{-2} be used for urban areas.

5. Evaluation of the model

The performance of LUMPS is evaluated using MUHD. Before doing so, we note that this approach contains both strengths and weaknesses. The merits are that the scheme is being tested against a comprehensive, high-quality dataset. Careful attention has been directed to the instrumentation, field methods, and quality control exercised in processing and analyzing the data. The dataset contains many of the essential surface and atmospheric characteristics of cities. The main weakness is that the same set used to develop some of the parameterizations (notably the relations for the α and β parameters—although model evaluation is conducted using hourly data while the parameter functions were derived using one average value for each site; Fig. 8a) is being used to test the overall operation of the combined scheme. The development of the dataset has been evolutionary, over a period of more than a decade; it is not now possible to extricate the data used to develop relations from those that were not. In the future, we aim to gather new sets, to use them to test LUMPS more independently, and to refine and extend parameterizations as the range of observational conditions (meteorological and surface cover) expands.

The evaluation is performed in a stepwise fashion to allow the impact of each modification on the performance of LUMPS to be considered independently. First, the original HPDM scheme is evaluated using MUHD (with two sets of parameters selected for α and β, respectively). Second, ΔQ_S is changed from the constant fraction 0.3Q^* (as used in HPDM) to the OHM scheme (see Table 1 for the values of coefficients used). Third, the new α relations (based on F_V and F_{lr}; see Table 5) are added, and the smaller value of β = 3 W m^{-2} is assigned. A summary of model runs, the combinations of schemes used, and a summary of the overall performance of the scheme (measured in terms of average root-mean-square error $\overline{\text{rmse}}$ across all sites) are given in Table 6. In all cases, the schemes are initialized with measured Q^*, and the fluxes are calculated on an hourly basis.

In this evaluation (except for run 13), each coefficient in LUMPS that is based on surface characteristics (i.e., a_1–a_3, α) is calculated for each hour of observation, based on the source area (footprint) of the measured turbulent flux [using the Schmid (1994) source area model]. Note that this is not a requirement of LUMPS;

here it simply ensures the greatest spatial consistency between the measured and modeled domains. The HPDM model is run with fixed values for all sites (Table 6). Run 13 evaluates LUMPS with fixed parameters for each site.

To evaluate the HPDM, and to consider the role of the α and β parameters, first the α parameter was changed from 0.5 to 1.0 (runs 1 and 2 in Table 6); these are the lower and higher default limits suggested for urban environments by the originators (Table 2). Measured ΔQ_S was used so the effect of the α and β parameters could be assessed independently. When α is increased, the results show a large increase in rmse when applied across all sites (from 30 to 88 W m^{-2} for both Q_H and Q_E). The lower value, used by Hanna and Chang (1992) in their analyses of sites in St. Louis, Missouri, and Indianapolis, Indiana, therefore gives much better performance. Using a constant fraction (0.3) of Q^* to calculate ΔQ_S reduces the performance of the HPDM: when $\alpha = 0.5$ (run 7) reductions are $\sim$27 W m^{-2} for Q_H and $\sim$6 W m^{-2} for Q_E. When $\alpha = 1.0$ (run 8), the model performance already is very poor, and it is degraded by 5–6 W m^{-2} for Q_E and Q_H.

Figures 9a (Q_H) and 9b (Q_E) are scatterplots showing the performance of HPDM ($\alpha = 0.5$, $\beta = 20$ W m^{-2}, $\Delta Q_S = 0.3Q^*$) for each of the individual cities in MUHD. At all sites, there is considerable scatter in the relation between measured and modeled values. HPDM underestimates the turbulent fluxes. In particular it misses Q_H at night and caps its maximum predicted values, resulting in underestimates during the middle of the day (Fig. 9a). There is a hysteresis pattern in the model discrepancies (most obvious in predictions of Q_H for Sg94). This is not directly evident to the reader from Fig. 9, but when the time of the points was added during analysis, hysteresis was distinct. The temporal nature of this error is due to the linear nature of the storage heat flux model used in HPDM (see discussion below).

Allowing the α parameter to vary dynamically as a function of F_V, rather than remaining constant at 0.5 (but with $\beta = 20$ W m^{-2} and measured ΔQ_S), results in a reduction of the rmse of 4 W m^{-2} ($\sim$7.5%; cf. runs 3 and 1 in Table 6). Modeling α as a function of F_{Ir} reduces the rmse by a further 2 W m^{-2} (cf. runs 4 and 3). Greater improvement in the performance of the model is derived by assigning a lower value to β (3 rather than 20 W m^{-2}); in response, the rmse drops by $\sim$6 W m^{-2} (cf. runs 5 and 3, 6 and 4). Lowering β has a significant effect at night (contrast Figs. 10 and 11 with Fig. 9). Thus we conclude that the revised methods for assigning α and β parameters presented here represent significant improvements over the use of fixed values for urban environments. The selection of F_V or F_{Ir} has a marginal effect. As indicated in section 4, the choice of this variable usually depends on data availability for a given site.

The approach taken to model ΔQ_S has a significant effect on overall model performance. When Q_H and Q_E are modeled with α as a function of area vegetated and $\beta = 3$ W m^{-2}, significant improvements are apparent with OHM as compared with the model with a constant fraction ($\Delta Q_S = 0.3Q^*$; cf. runs 11 and 9); across all cities the rmse drops by 10 W m^{-2} for Q_H and 3 W m^{-2} for Q_E. The city for which LUMPS performs least well is Tucson (Fig. 11). We believe this result is related to the fact that the Tucson site is exposed to the highest wind speeds of the cities in the database. Previous work concluded that OHM does least well in simulating ΔQ_S at this site (Grimmond and Oke 1999c). To illustrate the effects of OHM errors on Q_H and Q_E predictions, the model was rerun with measured ΔQ_S (cf. runs 11 and 5, and Figs. 10 and 11). When measured ΔQ_S is used, the rmse drops by 21 W m^{-2} for Q_H and by 7 W m^{-2} for Q_E, and the scatter for each of the cities (Fig. 11) is much reduced (Fig. 10). This result stresses the need for improvements in heat storage modeling in order to be able to parameterize accurately the turbulent fluxes, particularly in windy environments.

LUMPS is also run using fixed surface characteristics for each site (run 13; Table 7). These properties are calculated for circles around the respective sites. The radii of the circles are defined by generalized footprint analysis for the neutral case. The performance of LUMPS changes very little from the runs in which parameters are individually defined by complete flux source area analysis (see the results compared across the mean of the 12 sites in Table 6). The datasets that have the largest changes are the two Chicago sites and Sacramento (cf. Table 7 and Fig. 11). Even with fixed properties, LUMPS continues to show improvement over HPDM (contrast results in Table 7 and Fig. 9).

Overall, the results for LUMPS as presented here [$\alpha = f(F_V)$, $\beta = 3$ W m^{-2}, ΔQ_S from OHM] show the model performs well at many of the sites and is a significant improvement over former versions of HPDM.

6. Conclusions

Results of our local-scale surface energy balance observations reveal that turbulent sensible, latent, and storage heat fluxes all represent important terms in the surface energy balance of most cities. Each of the heat fluxes varies both spatially and temporally. Under the low-wind conditions so far studied, storage heat flux is most important at the downtown and light-industrial sites (at least 50% of daytime Q^*), and the sensible heat flux is most important at the residential sites (40%–60% of daytime Q^*). At the residential sites, latent heat flux, if sustained by garden irrigation and/or frequent rainfall, is also significant (20%–40% of daytime Q^*). Surface cover, notably the fraction of the surface vegetated and irrigated, exerts an important control on Q_E. At all sites, there is distinct hysteresis in the diurnal course of the storage heat flux; much more of the net radiation is used to heat the urban fabric in the morning. In addition, the

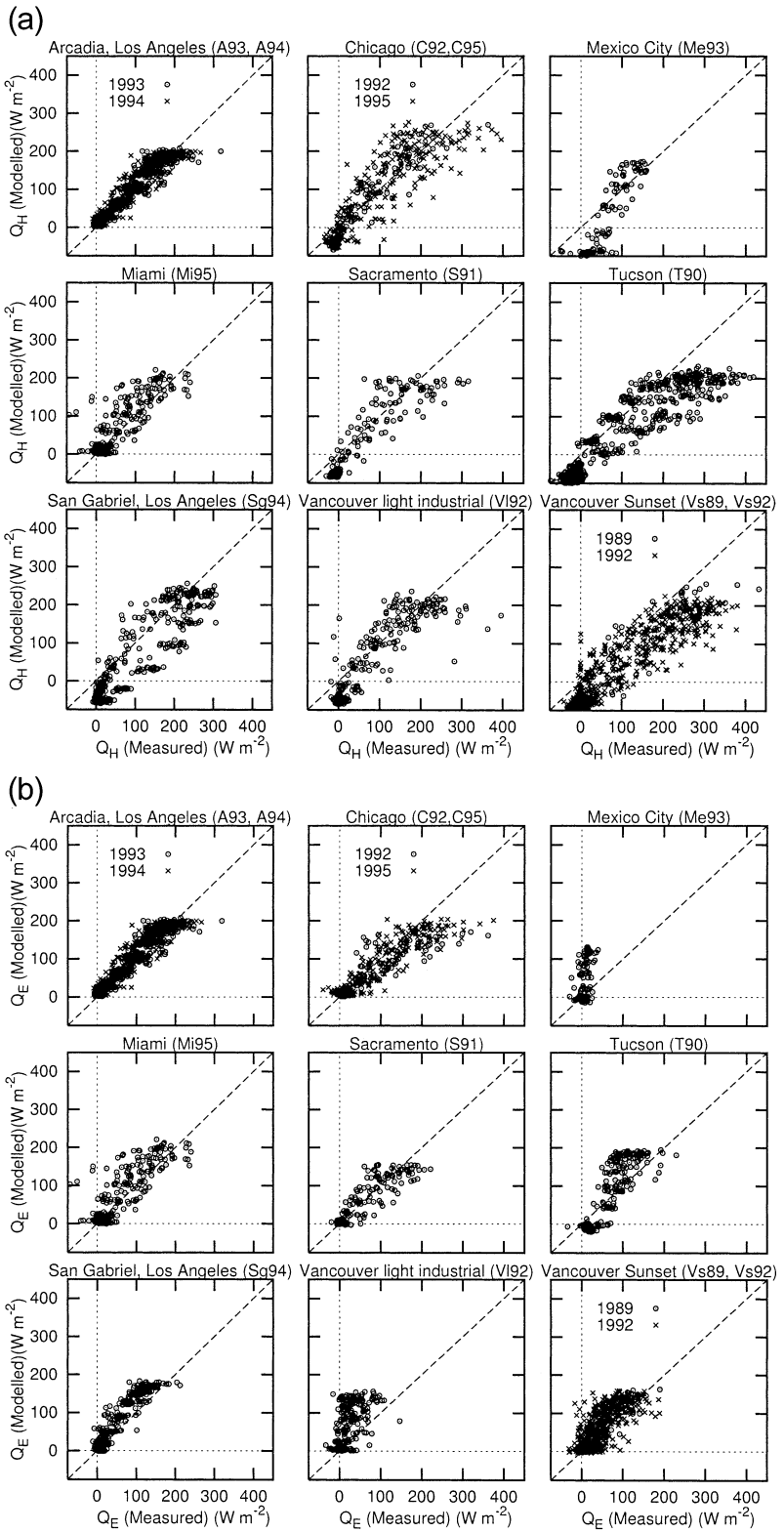

FIG. 9. Measured vs modeled (a) Q_H and (b) Q_E using HPDM with measured Q^*, $\Delta Q_S = 0.3Q^*$, $\alpha = 0.5$, and $\beta = 20$ W m^{-2} (run 7, Table 6).

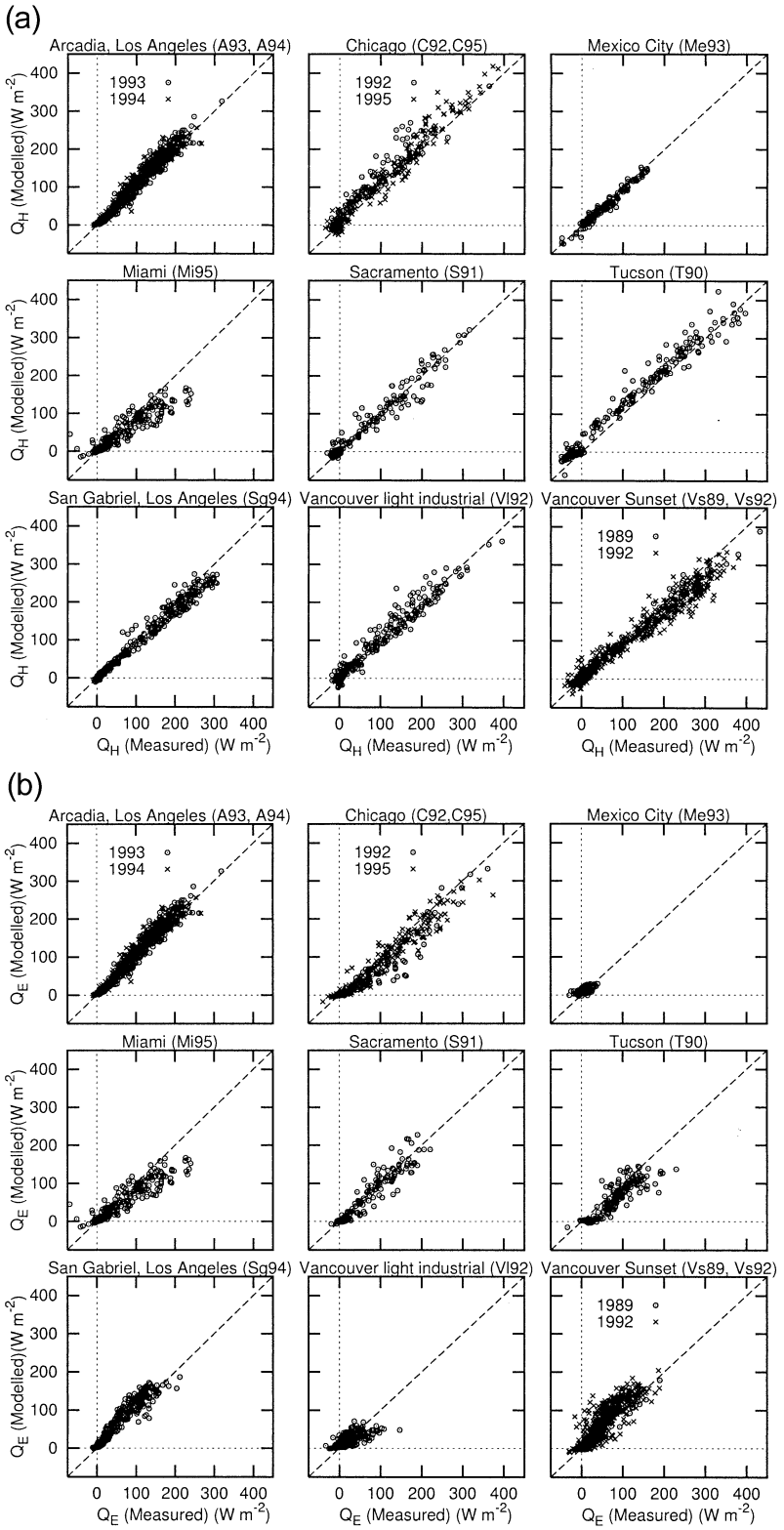

FIG. 10. Measured vs modeled (a) Q_H and (b) Q_E using measured Q^* and ΔQ_S with $\beta = 3$ W m^{-2} and α a function of F_V (run 5, Table 6).

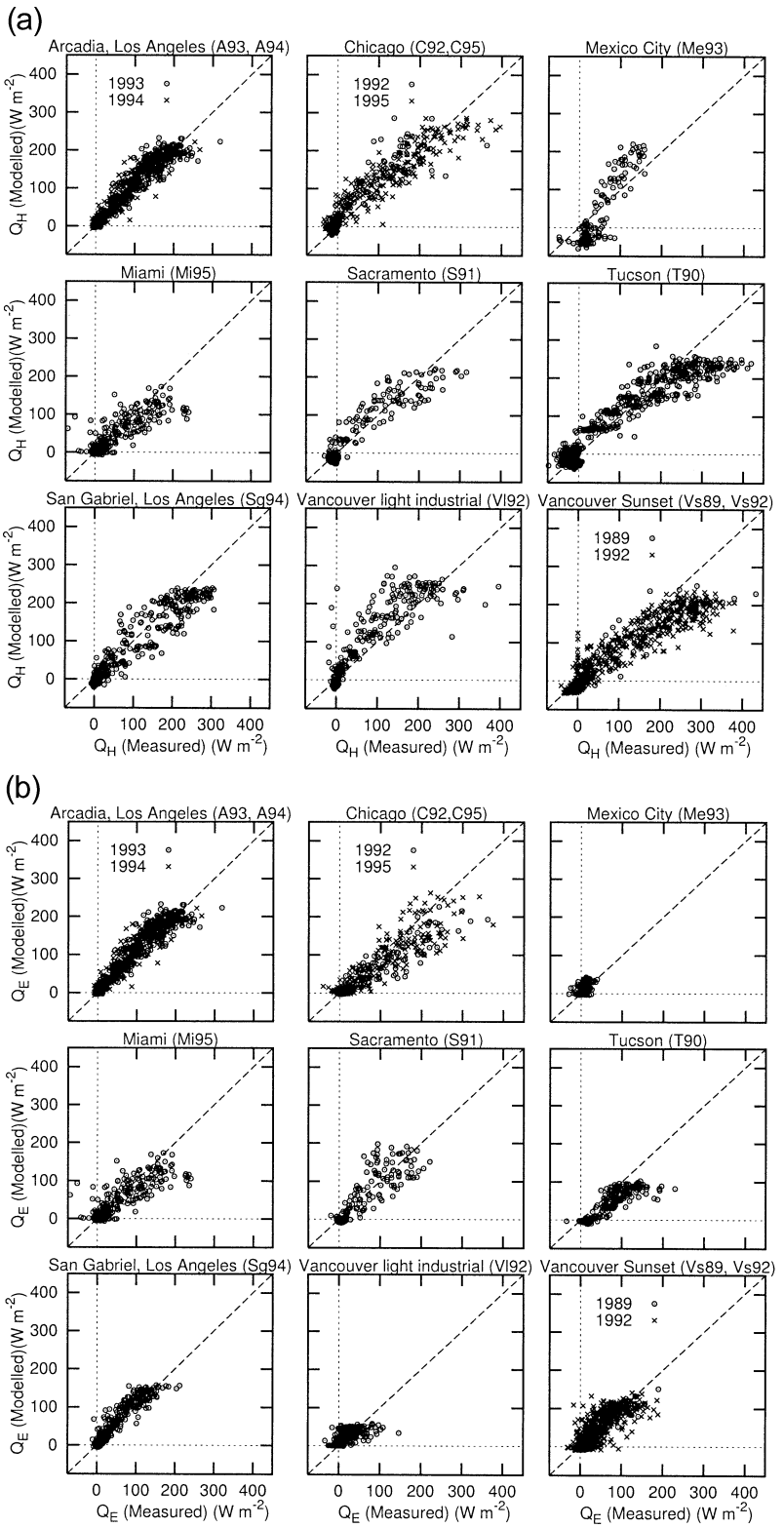

FIG. 11. Measured vs modeled (a) Q_H and (b) Q_E using LUMPS with measured Q^*, ΔQ_S from OHM, $\beta = 3$ W m^{-2}, and α a function of F_V (run 11, Table 6).

TABLE 7. Statistical results for measured vs modeled Q_H and Q_E using LUMPS with measured Q^*, ΔQs from OHM, $\beta = 3$ W m^{-2}, and α a function of F_V (run 13, Table 6). The surface characteristics are assigned fixed values for all time periods for each site. Compare with Fig. 9 (constant conditions for HPDM) and Fig. 11 (LUMPS but surface characteristics vary with source area characteristics for each hour).

	A93	A94	C95	C92	Me93	Mi95	S91	Sg94	T90	Vl92	Vs89	Vs92
Q_H												
Rmse	21	27	47	38	47	50	36	33	48	49	54	49
Rmse_{SY}	10	14	23	24	28	13	9	17	32	17	42	41
Rmse_{USY}	18	23	41	30	38	48	34	28	37	46	34	26
r^2	0.95	0.94	0.81	0.87	0.79	0.76	0.83	0.90	0.87	0.79	0.86	0.90
Q_E												
Rmse	19	20	42	58	14	30	24	16	38	20	21	25
Rmse_{SY}	5	7	35	51	6	17	8	3	33	13	12	5
Rmse_{USY}	18	19	23	26	12	25	23	15	17	15	17	24
r^2	0.93	0.93	0.87	0.69	0.20	0.77	0.85	0.90	0.77	0.38	0.85	0.67

sensible heat flux remains positive after the net all-wave radiation turns negative at night.

LUMPS, a simple local-scale urban meteorological parameterization scheme, is shown to be capable of predicting the 1D spatial and temporal variability in heat fluxes in urban areas. The data requirements for LUMPS are minimal: net radiation (which can be parameterized well from more routinely collected solar radiation), air temperature and humidity, atmospheric pressure, and surface descriptors (notably the plan-area fractions of vegetation, impervious surface, and roofs). The scheme represents an improvement over earlier models, such as HPDM. This improvement results largely from the OHM parameterization of storage heat flux, which takes into account both the magnitude of this flux and its hysteresis pattern, and new coefficients for the de Bruin and Holtslag (1982)/Holtslag and van Ulden (1983) equations, used to partition Q_H and Q_E, which now reflect urban green space and/or surface moisture availability and the positive Q_H fluxes observed in urban environments after sunset.

We readily acknowledge that there is plenty of scope for improvements in LUMPS; however, these likely will come at the expense of additional input requirements. We know that the effects of wind and large sources of anthropogenic heat are inadequately incorporated in the scheme. In situations in which these variables are important, LUMPS in its present form should not be used. In addition, because the observations in MUHD are collected by assuming a 1D energy balance, LUMPS is unlikely to perform well in areas of significant spatial variability of land cover and/or morphometry (for example, at the urban–rural edge, near coasts, or in complex terrain). MUHD also needs to incorporate vegetation phenology and winter conditions, including the effects of snow cover, melting, and freezing.

Acknowledgments. This research has been funded by the National Science Foundation, USDA Forest Service, Southern California Edison, Indiana University, the Natural Sciences and Engineering Research Council of Canada, and the Canadian Foundation for Climate and Atmospheric Science. The contributions of the many assistants and colleagues who aided in the collection of the field data on which our understanding is based are greatly appreciated. We also acknowledge the individuals and institutions who generously made field sites available. We thank Dr. Steve Hanna for his helpful comments on a draft of this paper.

REFERENCES

Beljaars, A. C. M., and A. A. M. Holtslag, 1989: A software library for the calculation of surface fluxes over land and sea. *Environ. Software,* **5,** 60–68.

——, and ——, 1991: Flux parameterization over land surfaces for atmospheric models. *J. Appl. Meteor.,* **30,** 327–341.

Cleugh, H. A., and T. R. Oke, 1986: Suburban–rural energy balance comparisons in summer for Vancouver, B.C. *Bound.-Layer Meteor.,* **36,** 351–369.

de Bruin, H. A. R., and A. A. M. Holtslag, 1982: A simple parameterization of surface fluxes of sensible and latent heat during daytime compared with the Penman–Monteith concept. *J. Appl. Meteor.,* **21,** 1610–1621.

de Haan, P., M. W. Rotach, and M. Werfeli, 2001: Modification of an operational dispersion model for urban applications. *J. Appl. Meteor.,* **40,** 864–879.

Ellefsen, R., 1990–91. Mapping and measuring buildings in the canopy boundary layer in ten U.S. cities. *Energy Build.,* **15–16,** 1025–1049.

Grimmond, C. S. B., 1992: The suburban energy balance: Methodological considerations and results for a mid-latitude west coast city under winter and spring conditions. *Int. J. Climatol.,* **12,** 481–497.

——, and T. R. Oke, 1986: Urban water balance. II: Results from a suburb of Vancouver, B.C. *Water Resour. Res.,* **22,** 1404–1412.

——, and C. Souch, 1994: Surface description for urban climate studies: A GIS based methodology. *Geocarto Int.,* **9,** 47–59.

——, and T. R. Oke, 1995: Comparison of heat fluxes from summertime observations in the suburbs of four North American cities. *J. Appl. Meteor.,* **34,** 873–889.

——, and ——, 1999a: Aerodynamic properties of urban areas derived from analysis of surface form. *J. Appl. Meteor.,* **38,** 1262–1292.

——, and ——, 1999b: Evapotranspiration rates in urban areas. *IAHS Publ.,* **259,** 235–243.

——, and ——, 1999c: Heat storage in urban areas: Observations and evaluation of a simple model. *J. Appl. Meteor.,* **38,** 922–940.

——, and ——, 2000: Heat fluxes and stability in cities. *Mixing Heights and Surface Energy Budget in Urban Areas: Proc. COST*

715 Expert Meeting, Antwerp, Belgium, European Commission (Rep. EUR 19447). [Available online at http://www.cordis.lu.]

——, H. A. Cleugh, and T. R. Oke, 1991: An objective urban heat storage model and its comparison with other schemes. *Atmos. Environ.,* **25B,** 311–326.

——, T. R. Oke, and H. A. Cleugh, 1993: The role of ''rural'' in comparisons of observed suburban–rural flux differences. *IAHS Publ.,* **212,** 165–174.

——, C. Souch, R. H. Grant, and G. Heisler, 1994: Local scale energy and water exchanges in a Chicago neighborhood. *Chicago's Urban Forest Ecosystem: Results of the Chicago Urban Forest Climate Project,* E. G. McPherson, D. J. Nowak, and R. A. Rowntree, Eds., USDA Forest Service Northeastern Forest Experiment Station, General Tech. Rep. NE-186, 41–61. [Available online at http://www.fs.fed.us/ne/home/publications/scanned/oldonline.html.]

——, ——, and M. Hubble, 1996: The influence of tree cover on summertime energy balance fluxes, San Gabriel Valley, Los Angeles. *Climate Res.,* **6,** 45–57.

Hanna, S. R., and J. C. Chang, 1992: Boundary layer parameterization for applied dispersion modeling over urban areas. *Bound.-Layer Meteor.,* **58,** 229–259.

——, and ——, 1993: Hybrid Plume Dispersion Model (HPDM) improvements and testing at three field sites. *Atmos. Environ.,* **27A,** 1491–1508.

Holtslag, A. A. M., and A. P. van Ulden, 1983: A simple scheme for daytime estimates of the surface fluxes from routine weather data. *J. Climate Appl. Meteor.,* **22,** 517–529.

King, T., and S. Grimmond, 1997: Transfer mechanisms over an urban surface for water vapor, sensible heat, and momentum. Preprints, *12th Symp. on Boundary Layers and Turbulence,* Vancouver, BC, Canada, Amer. Meteor. Soc., 455–456.

Meyn, S. K., 2000: Heat fluxes through roofs and their relevance to estimates of urban heat storage. M.S. thesis, Dept. of Geography, University of British Columbia, Vancouver, BC, Canada, 106 pp.

Newton, T., 1999: Energy balance fluxes in a subtropical city: Miami, FL. M.S. thesis, Dept. of Geography, University of British Columbia, Vancouver, BC, Canada, 140 pp.

Oke, T. R., 1988: The urban energy balance. *Prog. Phys. Geogr.,* **12,** 471–508.

——, 1997: Urban environments. *The Surface Climates of Canada,* W. G. Bailey, T. R. Oke, and W. R. Rouse, Eds., McGill-Queen's University Press, 303–327.

——, R. Spronken-Smith, E. Jauregui, and C. S. B. Grimmond, 1999: Recent energy balance observations in Mexico City. *Atmos. Environ.,* **33,** 3919–3930.

Rotach, M., 2000: The siting, choice and operation of surface instrumentation in urban areas. *Mixing Heights and Surface Energy Budget in Urban Areas: Proc. COST 715 Expert Meeting,* Antwerp, Belgium, European Commission (Rep. EUR 19447). [Available online at http://www.cordis.lu.]

Roth, M., and T. R. Oke, 1993: Turbulent transfer relationships over an urban surface. I: Spectral characteristics. *Quart. J. Roy. Meteor. Soc.,* **119,** 1071–1104.

Schmid, H. P., 1994: Source areas for scalars and scalar fluxes. *Bound.-Layer Meteor.,* **67,** 293–318.

Seibert, P., F. Beyrich, S.-E. Gryning, S. Joffre, A. Rasmussen, and P. Tercier, 2000: Review and intercomparison of operational methods for the determination of mixing height. *Atmos. Environ.,* **34,** 1001–1027.

Smith, S., 1994: 1992 Summer water balance. B. S. honours thesis, Dept. of Geography, University of British Columbia, Vancouver, BC, Canada, 82 pp. [Available from T. Oke at toke@geog.ubc.ca.]

Voogt, J. A., and C. S. B. Grimmond, 2000: Modeling surface sensible heat flux using surface radiative temperatures in a simple urban area. *J. Appl. Meteor.,* **39,** 1679–1699.

Yap, D. H., 1973: Sensible heat fluxes in and near Vancouver B.C. Ph.D. thesis, Dept. of Geography, University of British Columbia, Vancouver, BC, Canada, 177 pp.